Applied Nanoscience (2019) 9:2091–2102
https://doi.org/10.1007/s13204-019-01026-0

ORIGINAL ARTICLE

Growth mechanism identification of sputtered single crystalline bismuth nanowire

Haiyang Hong[1] · Lu Zhang[1] · Chunyu Yu[1] · Ziqi Zhang[1] · Cheng Li[1] · Songyan Chen[1] · Wei Huang[1] · Jianyuan Wang[1] · Jianfang Xu[1]

Received: 13 February 2019 / Accepted: 2 April 2019 / Published online: 9 April 2019

Abstract
Single crystalline bismuth nanowire is recently considered as one of the most attractive low dimensional materials for the exploration of exotic higher-order topological properties. However, its growth mechanism by sputtering, which is regarded as one of the most cost-effective and simplest method, is still unrevealed. In this work, a bismuth nanowire growth model based on surface diffusion driven by chemical potential difference among crystal facets is proposed for sputtering method. The morphology evolution of bismuth nanowires is captured for the first time, and three corresponding growth stages are clearly discriminated. The possible self-catalyzed, stress-driven, and screw dislocation-driven nanowire growth mechanisms are precluded separately based on the theoretical and experimental data. The thoroughly understanding of growth mechanism is fundamental and necessary for fabrication of size-controllable bismuth nanowires and may pave the way for the preparation of other low dimensional materials and the investigation of novel physics.

Keywords Bismuth · Nanowire · Sputtering · Surface diffusion · Single crystalline

Introduction

Bismuth has intrigued great interest recently for its novel feature as higher-order topological insulator, in which gapless topological states protected by special symmetries exist at corners or hinges, while the edges and surfaces are gapped in two- and three-dimensional systems, respectively (Schindler et al. 2018a, b; Benalcazar et al. 2017). In the past, various experiments for the investigation of bismuth electronic structure have been carried out, revealing exciting features such as one-dimensional topological modes localized along step edges (Drozdov et al. 2014), conducting hinge channels (Li et al. 2014; Murani et al. 2017), and quantum spin Hall effect (Murakami 2006). Among the experiments, bismuth nanowire is presented to be vital for the exploration of peculiar one-dimensional electrical conduction modes and the application of dissipationless electronic devices in the future. Therefore, an effective and simple method to fabricate high crystalline bismuth nanowire is essential for paving the way of investigating the higher-order topological feature. Several preparation methods have been performed such as solvothermal process (Liu et al. 2003), electrochemical deposition with anodized aluminum template process (Liu et al. 1998; Li et al. 2003), pressure injection process (Lin et al. 2000), stress-induced process (Shim et al. 2009; Cheng et al. 2002), and sputtering process (Cao et al. 2009; Stanley et al. 2012; Tian et al. 2012; Lee et al. 2013). Among the proposed methods, sputtering is regarded as the most cost-effective and simplest method to acquire large amount of single crystalline bismuth nanowires with controllable wire length and diameter. However, the intrinsic growth mechanism of bismuth nanowire by sputtering is still in puzzle. A few explanations based on incomplete clues, e.g., spiral growth driven by screw dislocation (Shim et al. 2009), lead to misleading interpretations.

In this work, the morphology, crystallinity, and growth mechanism of bismuth nanowire grown by sputtering are thoroughly investigated. Scanning electron microscope (SEM), high-resolution transmission electron microscope (HRTEM) and selective area electron diffraction (SAED) are used for the characterization of the morphology evolution

✉ Cheng Li
lich@xmu.edu.cn

[1] Semiconductor Photonics Research Center, OSED, Department of Physics, Jiujiang Research Institute, Xiamen University, Xiamen 361005, Fujian, People's Republic of China

and crystallinity of bismuth nanowire, respectively. Three growth stages are discriminated for the first time. Based on experimental and theoretical analyses, the growth mechanism of bismuth nanowire by sputtering is unambiguously proposed. In addition, other possible mechanisms for nanowire growth (Shim et al. 2009; Tian et al. 2012; Woo et al. 2009; Bierman et al. 2008) are reasonably precluded.

Experimental

The syntheses processes were carried out by DC magnetron sputtering with oxidized silicon substrates and 99.99% pure bismuth target. To begin with, silicon substrates with top 800 nm SiO_2 were cleaned by acetone followed by ethyl alcohol with ultra-sonic for three cycles and finally rinsed in deionized water for times. After drying, the substrates were immediately transferred into the magnetron sputtering chamber and the ambient pressure was pumped to 10^{-4} Pa. In the purpose of identifying the mechanisms in the formation of bismuth nanowires, several parameters for the deposition were adjusted.

In the first group, the sputtering durations were set as 0.33, 1, 3, 4, 5, 6, 10, 30, 60, and 90 min. The sputtering pressure, power, and substrate temperature were kept at 0.5 Pa, 7.80 W, and 150 °C, respectively. This group was denoted as Time-varying group. In the second group, the substrate temperatures were set as room temperature (RT), 100, and 150 °C. The sputtering pressure, power, and duration were kept at 0.5 Pa, 7.80 W, and 10 min, respectively. This group was denoted as temperature-varying group. In the third group, the sputtering pressure was set as 0.5, 1.0, and 1.5 Pa. The sputtering power, duration, and substrate temperature were kept at 7.80 W, 10 min, and 150 °C, respectively. This group was denoted as pressure-varying group. In the last group, the sputtering power was set as 2.40, 7.80, 17.16, and 33.19 W. The sputtering pressure, duration, and substrate temperature were kept at 0.5 Pa, 10 min, and 150 °C, respectively. This group was denoted as power-varying group. More intuitive classification can be seen in Table 1.

Results and discussion

The morphology evolution of deposited samples in time-varying group

As the SEM images shown in Fig. 1a, the sputtered bismuth atoms form as nanoscale clusters separately rather than a thin film after 0.33 min deposition. In the 1-min sputtering sample, the clusters grow up while still be isolated with each other. As the sputtering time increases to 3 min, a thin film with relatively smooth surface is formed although some narrow gaps are distributed uniformly on it. This is attributed to the further growth of the clusters, where adjacent clusters merge or squeeze the gap. In the 4-min sputtering sample, a denser film takes shape with less and narrower gaps. Particularly, as the time increase to 5 min, rod-like and hillock-like objects are formed simultaneously on the surface of gapless film. Merely one more minute deposition, as shown in the 6-min sputtering sample, the length of nanoscale rod-like objects extends to a few microns and the size of hillock-like objects becomes bigger. In addition, grain shape particles are developed meanwhile. In the 10-min sputtering sample, nanowires with large aspect ratio are formed as a consequence of continuous growth of rod-like objects. And both the lengths of the nanowires and the size of the hillocks-like objects increase as the sputtering time prolongs to 30, 60, and 90 min. For a comprehensive characterization of morphology, a typical cross-sectional view taken by SEM is provided. As shown in Fig. 1b, the as-grown nanowires are obliquely standing on the film with uneven length distribution. Besides, the film is consisted of abutting rod-like grains as shown in the inset SEM image on the right top. Therefore, the morphology evolution of deposited sample in Time-varying group can be classified into three stages as follows: (i) film formation; (ii) nanowire and hillocks growing; (iii) nanowire ripening. Furthermore, quantitative analyses based on statistics are carried out for the determination of the growth mechanism. As the black rectangle dot line depicted in Fig. 1a, the mean length of bismuth nanowire increases with sputtering time and becomes almost saturated as the time beyond 60 min. The vertical bar presents the statistic

Table 1 Experimental groups classification and corresponding sputtering parameters

Parameters	Time (min)	Temperature (°C)	Pressure (Pa)	Power (W)
Groups				
Time-varying	0.33, 1, 3, 4, 5, 6, 10, 30, 60, 90	150	0.5	7.80
Temperature-varying	10	RT, 100, 150	0.5	7.80
Pressure-varying	10	150	0.5, 1.0, 1.5	7.80
Power-varying	10	150	0.5	2.40, 7.80, 17.16, 33.19

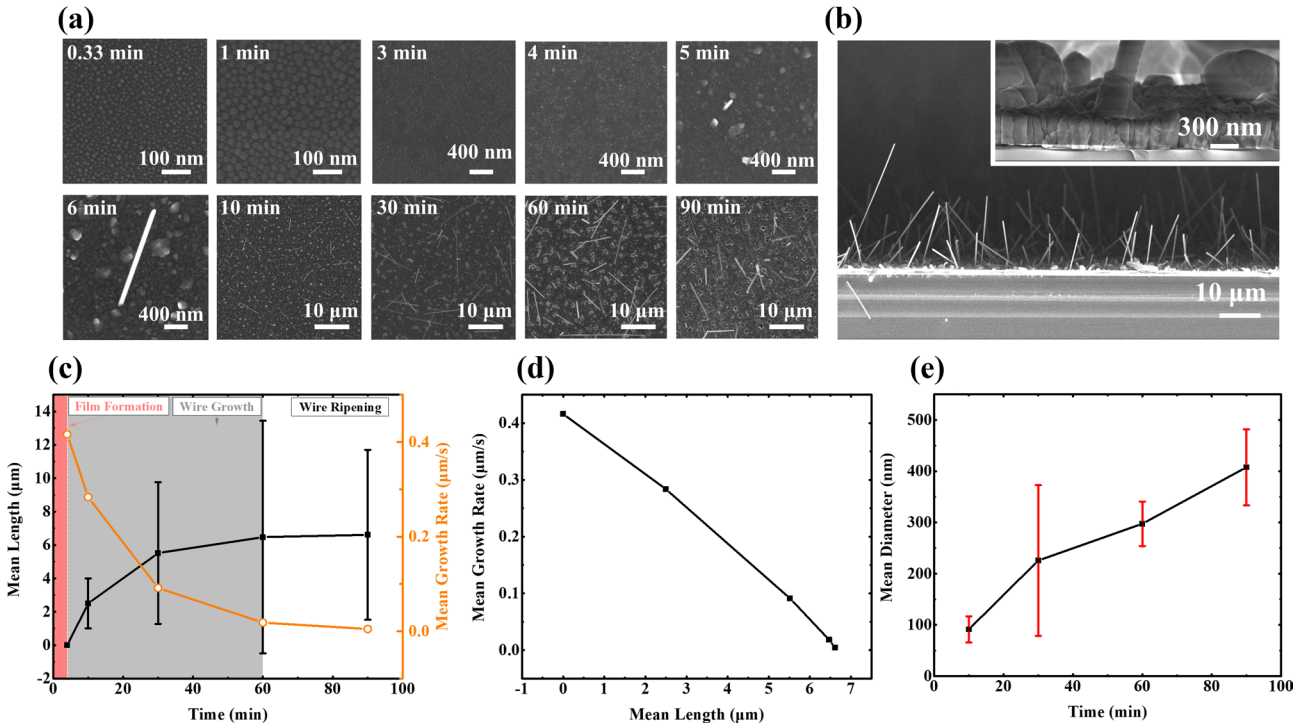

Fig. 1 **a** SEM images of the morphology evolution in Time-varying group, the vertical bar presents the statistic standard error. **b** Typical cross-sectional view of as sputtered sample with grown bismuth nanowires, and a layer of bismuth film consisted of jointed columnar bismuth grains supports the standing nanowires as shown in the inset on the top right. **c** The nanowire's mean length (shown in black rectangle solid dot line) and mean growth rate (shown in yellow open circle line) dependence on the sputtering time. **d** The mean growth rate dependence on mean length. **e** The relationship between mean diameter of bismuth nanowire and sputtering time

standard error. The film formation, nanowire growing, and nanowire ripening regimes are colored in pink, grey, and white, respectively. By differentiating the time dependent mean length line, we can acquire the relationship between the nanowire's mean growth rate and sputtering time, as the open yellow circle line shown in Fig. 1c. The mean growth rate is inversely proportional to the deposition time in an exponential behavior, indicating a non-uniform growth. Moreover, the mean growth rate decreases sub-linearly with respected to the nanowires' mean length as shown in Fig. 1d, manifesting a strongly wire length-related nanowire growth mechanism. Differently, a uniform growth behavior of the mean diameter of the nanowires is shown in Fig. 1e, and not any saturated regime is observed. Accordingly, a non-uniform growth in the nanowire's axis direction, where the growth rate is fast at the initial stage and slow at the later stage of the nanowire growing regime, and a uniform growth in the nanowire's radial direction are demonstrated.

The morphology variation of deposited samples in temperature-varying group

As shown in Fig. 2a, the surface topography of all samples is similar with nanowires and hillocks presence. However, variations are observed as shown in Fig. 2b, c. In Fig. 2b, the mean length of the nanowires increases linearly with the substrate temperature. And in Fig. 2c, the mean diameter of the nanowires also tends to increase with the substrate temperature, although the slightly deviation from the line may be attributed to the measurement error. Therefore, both the mean length and mean diameter of the nanowires approximately increase uniformly with the rise of substrate temperature.

The morphology variation of deposited samples in pressure-varying group

In Fig. 3a, the nanowires and hillocks dramatically decrease as the sputtering pressure increase from 0.5 to 1.5 Pa as the top row SEM images shows, and the roughness of the deposited film is reduced as shown in the down row images. The mean length of the nanowires decreases linearly with the increase in pressure, as shown in Fig. 3b, and reaches zero at 1.5 Pa. Nevertheless, the mean diameter of the nanowires decreases sub-linearly with the pressure and becomes zero either. These phenomena indicate the inhabitation of the pressure increase for the growth of nanowire and not any

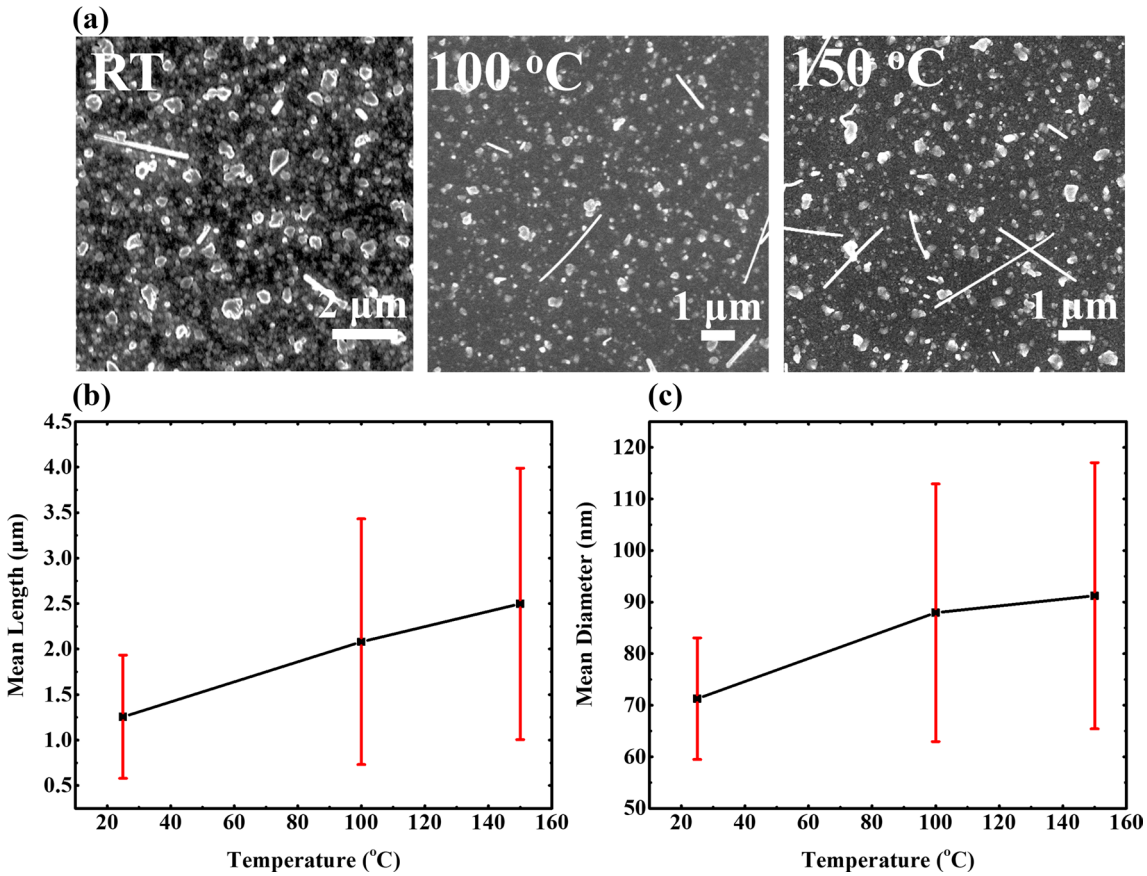

Fig. 2 **a** SEM images of the morphology variation in temperature-varying group. Substrate temperature dependent variation of **b** the mean length and **c** the mean diameter of bismuth nanowire

nanowire is generated at 1.5 Pa. And dramatic decrease in the mean diameters to zero sub-linearly is due to the discontinuous change in nanowire diameter at the critical point of nanowire growth.

The morphology variation of deposited samples in power-varying group

As shown in Fig. 4a, narrow-gaps distributed film without any nanowires and hillocks is presented at 2.40 W sputtering power, where the morphology is similar to that of the 3 min sample in time-varying group. This is because the amount of deposited atoms is not enough for the formation of a continuous film, as the sputtering energy is 2.40 W × 600 s = 1440 J approximately equals to 7.80 W × 180 s = 1404 J in 3 min sample of time-varying group. As the power increases to 7.80 and 17.16 W, both nanowires and hillocks are formed. However, as the power rises to 33.19 W, reductions of nanowire's length and hillock's size occur. In Fig. 4b, the mean length of the nanowires increases nonlinearly with the increase in sputtering power and maximizes at 17.16 W, while decreases as the power continuing to increase. For mean diameter of the nanowires, sub-linear dependence on sputtering power can be clearly observed in Fig. 4c, as shown in black dot line. However, in the nanowire presence regions, the relationship of mean diameter between sputtering power is almost linear. By fitting, a line in red agrees well with the measured points and shows large difference with the measured data at 2.40 W. It can also be well interpreted by the discontinuous change in nanowire diameter at the critical point of nanowire growth as discussed in pressure-varying group. Consequently, increasing the sputtering power within a moderate range promotes the growth of nanowire while attenuation takes place as the power further increases. However, the mean diameter of the nanowires is supposed to extend linearly with the increase in power. All the morphology variations respected to the corresponding variates in the four groups are summarized in Table 2.

Crystallinity characterization of the deposited nanowires

As shown in Fig. 5a, the HRTEM images of the nanowire's tip, where the black arrow point from Fig. 5b, clearly show

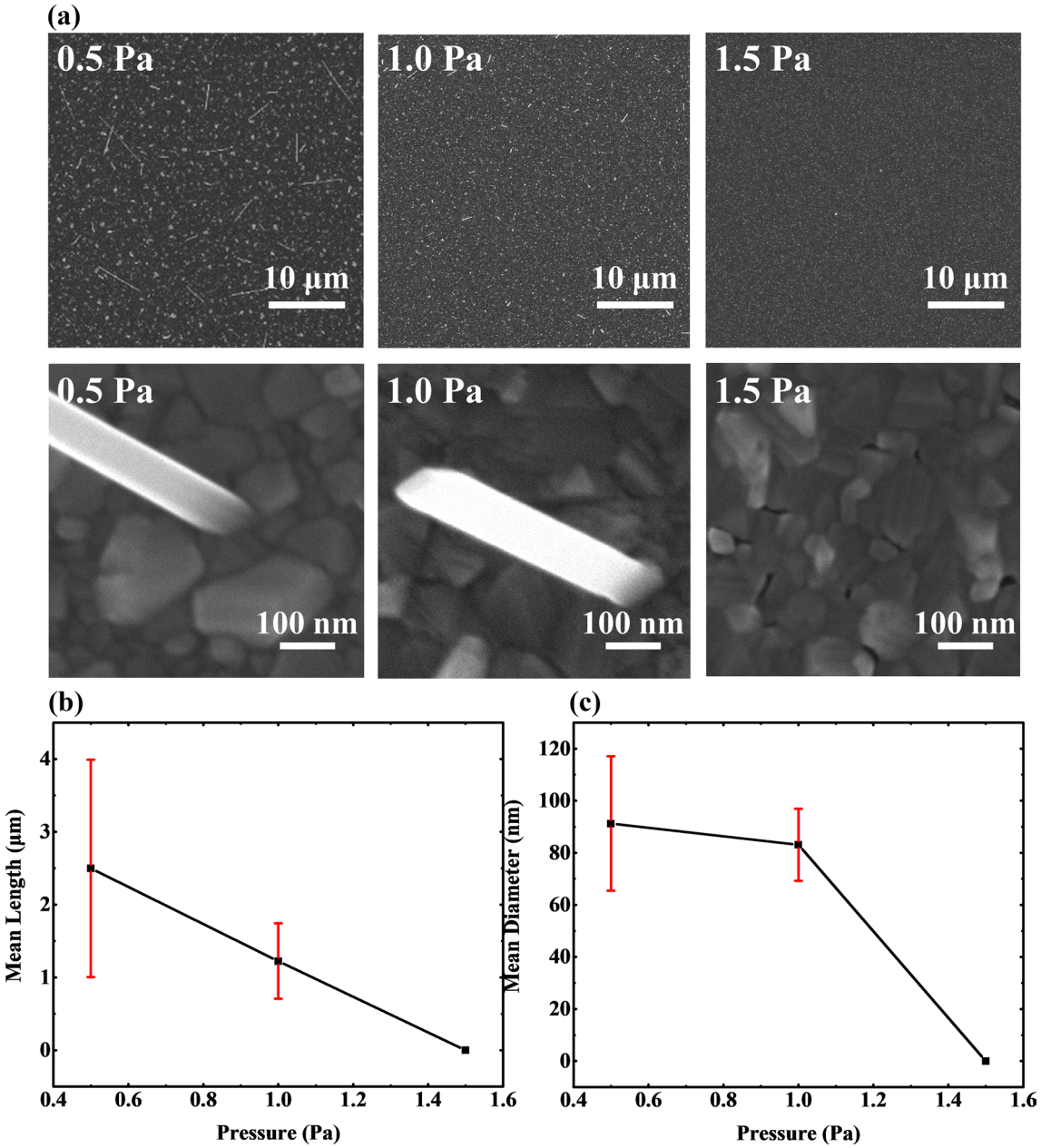

Fig. 3 **a** SEM images of the morphology variation in pressure-varying group. Sputtering pressure dependent variation of **b** the mean length and **c** the mean diameter of bismuth nanowire

uniform lattice and the inter-planar distance in the nanowire's axis direction is measured to be 2.2673 Å. Compared with Fig. 5c, d HRTEM images of selected areas, we can unambiguously observe that all the lattice of the selected areas of the nanowire are intact and consistent with each other with the nanowire orienting [110] direction in hexagonal lattice. Furthermore, as the SAED images shown in Fig. 5e, a perfect electron diffraction pattern is performed, indicating high single crystalline of the bismuth nanowire. The axis direction is calculated to be in line with the results from HRTEM. It should be noted that the features of the bismuth nanowire as shown are typical for the wires as obtained. Therefore, the bismuth nanowire prepared in this work is single crystalline with preferred [110] orientation.

Identification of growth mechanisms of bismuth nanowire deposited by sputtering

As has been discussed in Time-varying group, before the growth of bismuth nanowire, a continuous bismuth film is required. This precondition coincides with that of on-film

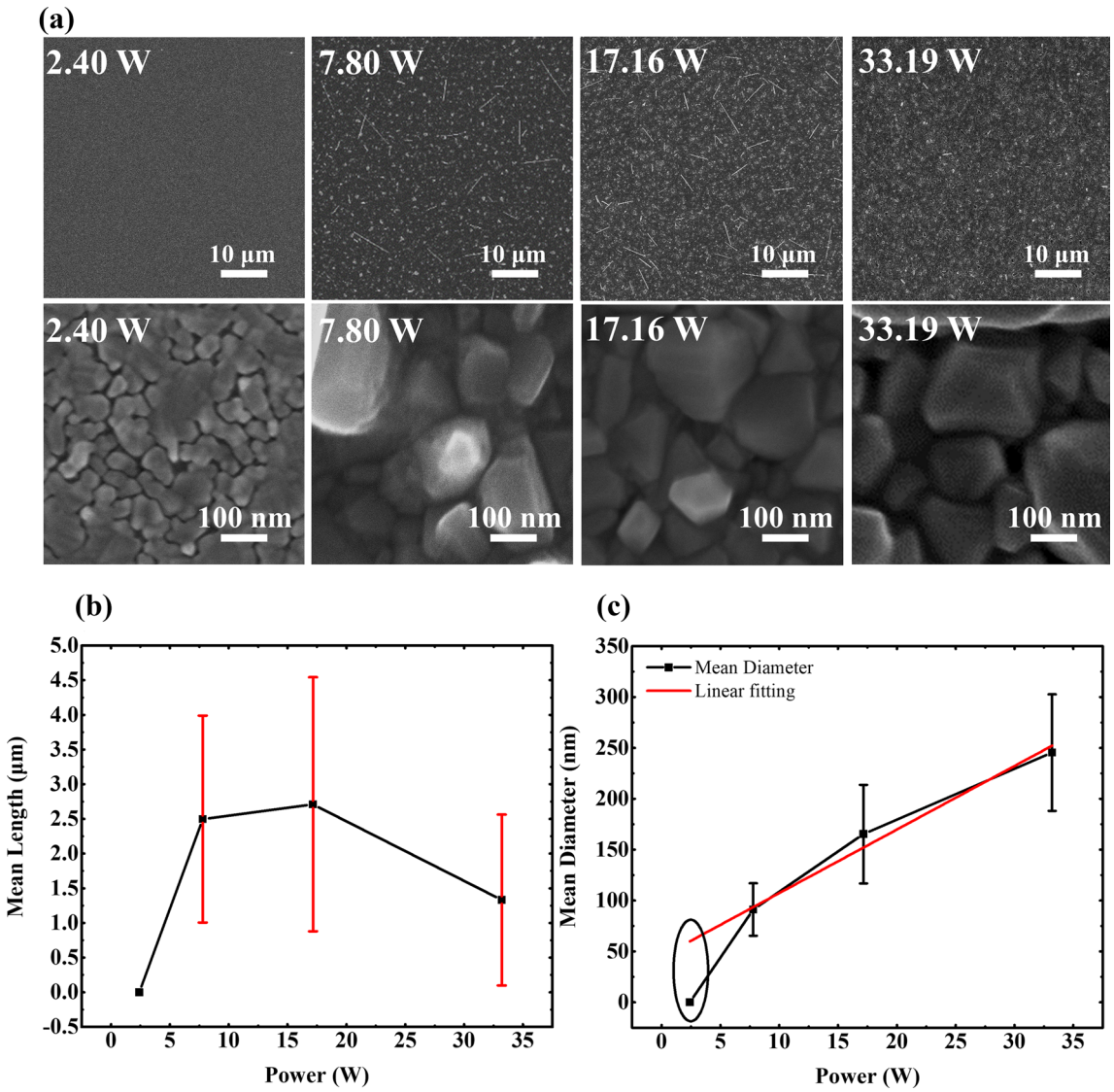

Fig. 4 **a** SEM images of the morphology variation in power-varying group. Sputtering power dependent variation of **b** the mean length and **c** the mean diameter of bismuth nanowire with a linear fitting performed between 7.80 and 33.19 W, and larger than 50 nm mean diameter is extrapolated at 2.40 W, as marked by black ellipse

Table 2 The tendency of bismuth nanowire's mean length and mean diameter with respected variates in time-varying, temperature-varying, pressure-varying, and power-varying groups, and the dependence of mean growth rate on sputtering time and length of nanowire in time-varying group are presented

Parameters	Mean length v.s. variate (increase)	Mean diameter v.s. variate (increase)	Mean growth rate v.s. time (increase)	Mean growth rate v.s. mean length (increase)
Groups				
Time-varying	Increases sub-linearly and nearly saturates beyond 60 min	Increases linearly	Decreases exponentially	Decreases sub-linearly
Temperature-varying	Increases linearly	Increases linearly	–	–
Pressure-varying	Decreases linearly	Decreases linearly	–	–
Power-varying	Increases sub-linearly within 17.16 W, decreases beyond 17.16 W	Increases linearly	–	–

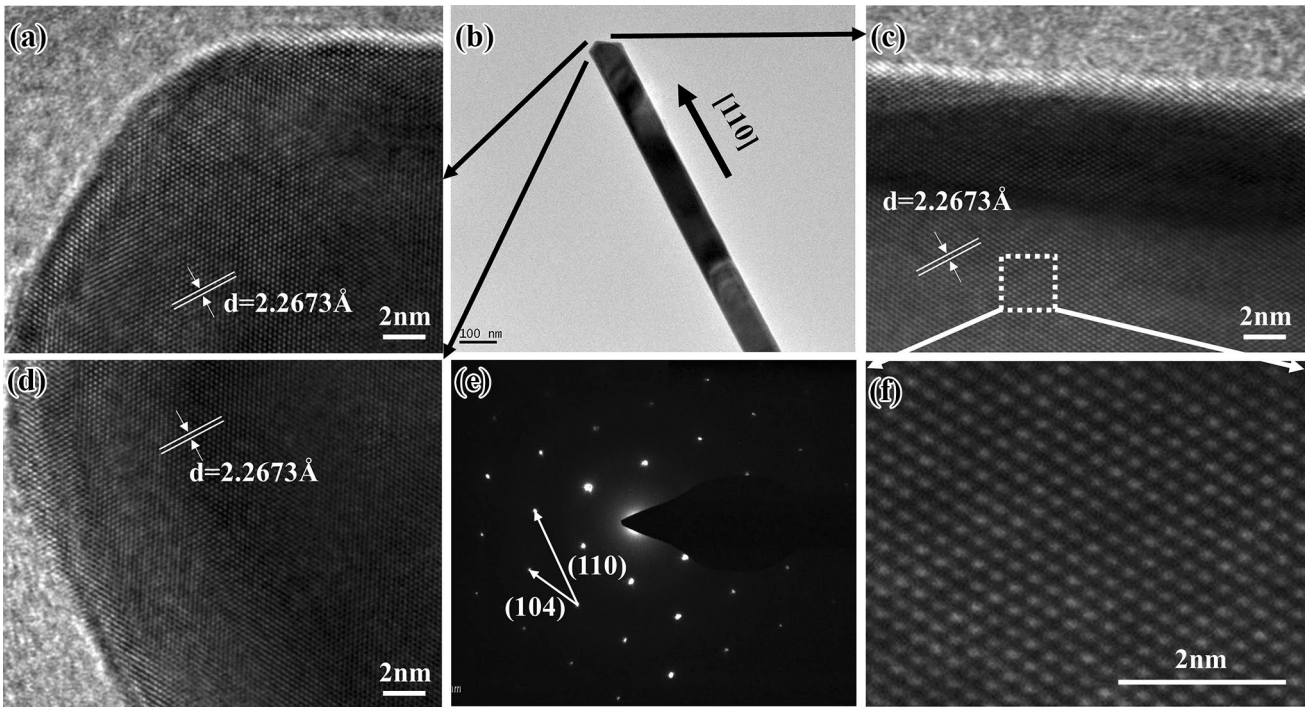

Fig. 5 The TEM images of bismuth nanowire, **a** at top tip area, **b** overall morphology, **c** at tip side, **d** at nanowire up left sidewall, and **e** the SAED pattern of the nanowire. **f** The HRTEM image of the selected area from **c** as circled in a dash square

formation of nanowire (OFF–ON) method proposed by Shim et al. (2009). However, the inherent growth mechanism of bismuth nanowire in this work is totally different. The driving force in OFF–ON method is compress strain which resulted from the difference of thermal expansion coefficient between bismuth film and substrate. Therefore, the growth front lies at the nanowire's root, and the nanowire's tip remains unchanged once grown. Moreover, nanowire can only be extruded from grain boundary for the relaxation of stress. However, the nanowire's growth front in our work is demonstrated to lie at the tip of bismuth nanowire. As shown in Fig. 6a–d, all the crossovers are consisted of two jointed bismuth nanowires with one of the nanowires indents at the cross point. Particularly, by detaching the crossover, as shown in Fig. 6d, an arched notch can be seen at the indented bismuth nanowire. Furthermore, the bismuth nanowire not only grows directly from the bismuth film but also from the hillock as shown in Fig. 6e, f, respectively, whereas nanowires prepared by OFF–ON method only extrudes from the bismuth film instead of hillocks, where the stress is negligible. As a result, the deformation of the indented nanowire and the hillock-base of bismuth nanowire preclude the stress induced growth mechanism as proposed in OFF–ON method and demonstrates the tip's growth behavior. To determine the growth mechanism of bismuth nanowire, the theoretical steady-state bismuth morphology is performed by Bravais–Friedel–Donnay–Harker (BFDH) principle (Docherty et al. 1991). Bismuth crystal forms a structure in space group $R\bar{3}m$ with rhombohedral symmetry as shown in the left of Fig. 7a. Three equidistant nearest-neighbor atoms and three equidistant next-nearest neighbors slightly further away for each atom. This results in puckered bilayers of atoms, as shown in the middle of Fig. 7a, perpendicular to the hexagonal [001] direction where each atom is covalently bonded to its three nearest atoms. The next-nearest atoms are in the adjacent bilayer and the bonding of inter-bilayer is much weaker than that within each layer. According to BFDH principle, the preferred morphology shows [110] oriented hexagonal prisms with four facets closed tip, shown in the right of Fig. 7a. The side facets include (003), (1–12), and (1–1–1) while the tips facets consist of (101), (012), (01–1), and (10–2). This predicted morphology is completely consistent with the HRTEM characterization. In the view of crystallography, the shortest facets distance and maximum number of inter-planar covalence bonds of (110) among the facets ensure the lowest facet free energy and facilitate the highest growth rate along [110] direction. Therefore, growth of bismuth nanowire on bismuth grain with [110] direction outward is possible. For the determination of whether the growth of bismuth nanowire is motivated merely by direct sputtering atoms, two-step sputtering is carried out. As shown in Fig. 7c, a substrate with isolated bismuth grains is prepared after 5 min sputtering on substrate at 250 °C. Cooling in vacuum to 150 °C, a continuous bismuth film without

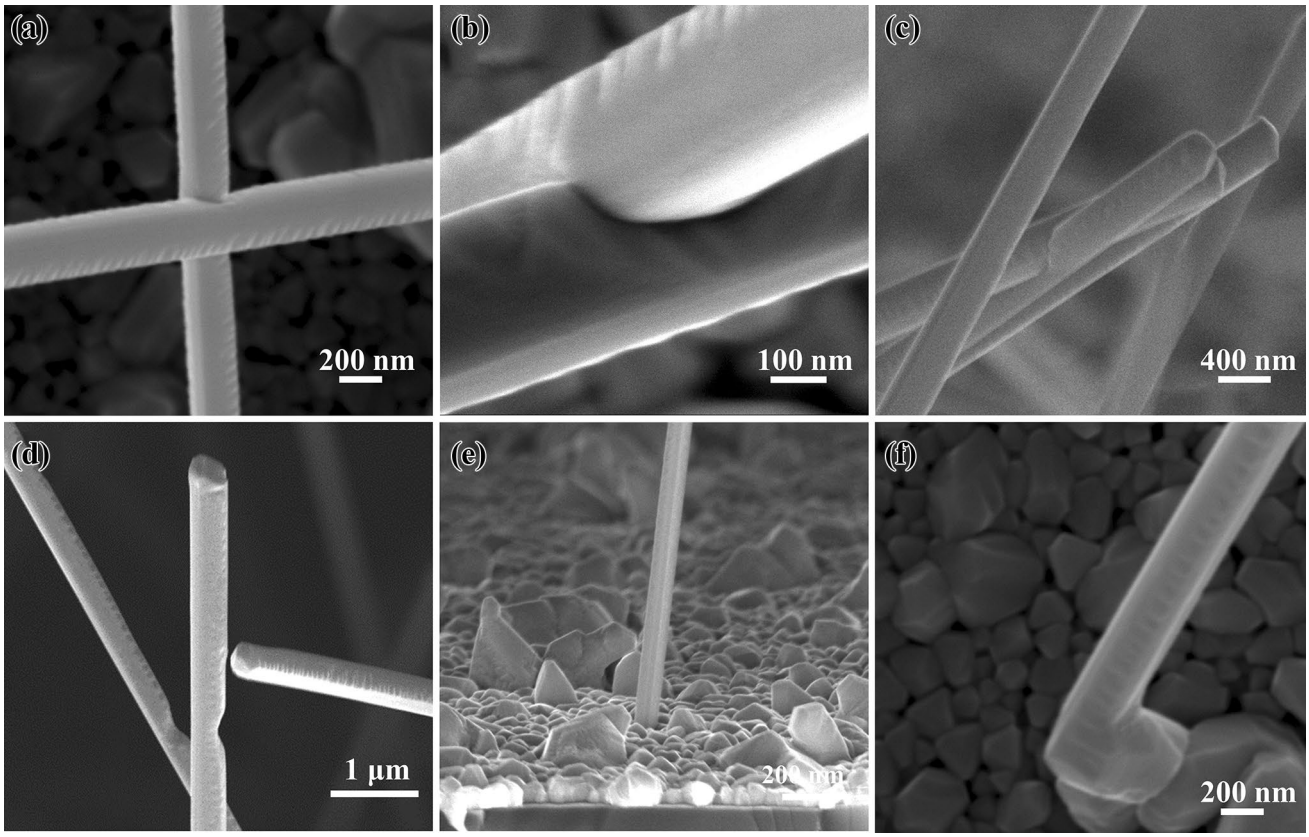

Fig. 6 The SEM images of **a**–**c** intersected bismuth nanowires, **d** mechanically detached crossover of bismuth nanowires, and the growth of bismuth nanowire **e** from the bismuth film and **f** from the hillock

any bismuth nanowire is formed after another 5 min sputtering, as shown in Fig. 7d. The pressure and power of the two-step sputtering are 0.5 Pa and 7.80 W, respectively. The grainy substrate is supposed to be consisted of grains with various orientation outward including [110]. However, gap filling without film thickness increase instead of nanowire growth is observed. Therefore, there must be a migration of the second time sputtered bismuth atoms. Actually, the chemical potential in gaps of the film is lower than that of the film's top surface (Floro et al. 2002; Chason et al. 2002) and even lower than (110) plane in this work. However, migration of condensed atoms is improbable because extra energy is needed for the break of chemical bonds.

Based on the results above, surface bismuth adatoms diffusion is supposed to be responsible for the atoms migration and the formation of bismuth nanowire. At the beginning of film formation stage, as shown in Fig. 8a, the bismuth adatoms on the substrate tend to assemble into clusters for the minimization of free energy due to the Gibbs free energy equation, $\Delta G = -N\Delta\mu + \sigma S$, where N denotes the number of atoms, $\Delta\mu$ the chemical potential difference between the mother and offspring phase, σ the surface free energy per unite area of the offspring surface, and S the total area of the offspring surfaces. Since the first term $-N\Delta\mu$ being consistent, the ΔG depends only on the second term σS and maximizes when S is minimum. In this case, the sputtered bismuth atoms are energetic favorably gathered with each other to form clusters rather than an ultra-thin film, where the surface area would be larger than that of the clusters in such a small number of atoms. Continue to sputtering, the clusters expand and meet with each other to merge or to form grain boundaries, leaving a relatively smooth bismuth film as schematically depicted in Fig. 8b. Since the chemical potential at the grain boundary is the lowest, adatoms are energetic favorably diffuse into the grain boundary leading to an excess number of atoms allowed in the gap, resulting compress strain nature of the film. In consequence, a film is preformed and hillocks are generated to release the stress. It is worth noting that the diffusion of bismuth adatoms is driven directly by the adatoms concentration gradient which induced by the difference of surface chemical potential. At the meantime of film formation, grains with (110) plane oriented out of the surface attract adatoms nearby in a range within the diffusion length λ_s of bismuth adatoms on the surface for a lower surface free energy of (110) plane as compared to that of film surface. As shown in Fig. 8c, the

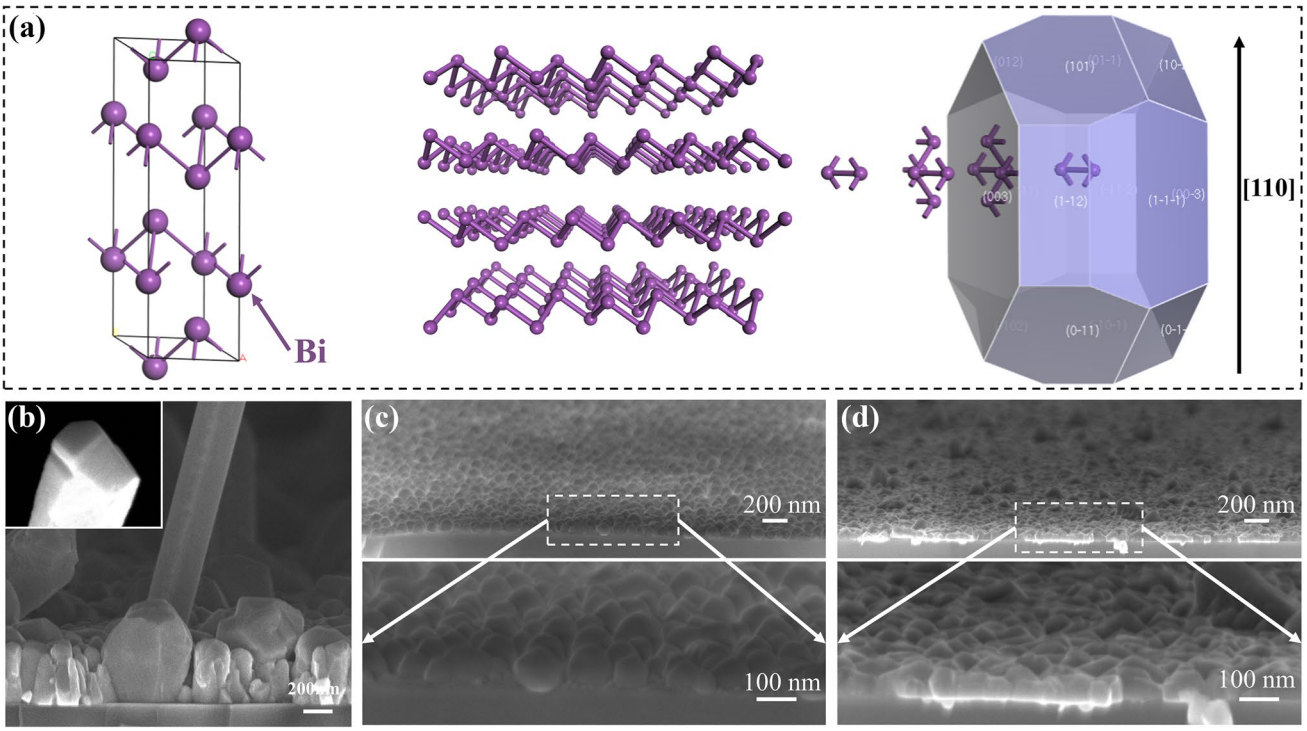

Fig. 7 **a** The cell structure (left), bulk structure (middle), and preferential crystal shape (right) of bismuth. The cross-sectional SEM image of **b** as deposited bismuth sample with clearly four facets closed tip morphology as the inset shows on the top left, **c** 5 min sputtering with substrate temperature 250 °C, and **d** another 5 min in-situ sputtering on the substrate in (**c**) with substrate temperature 150 °C

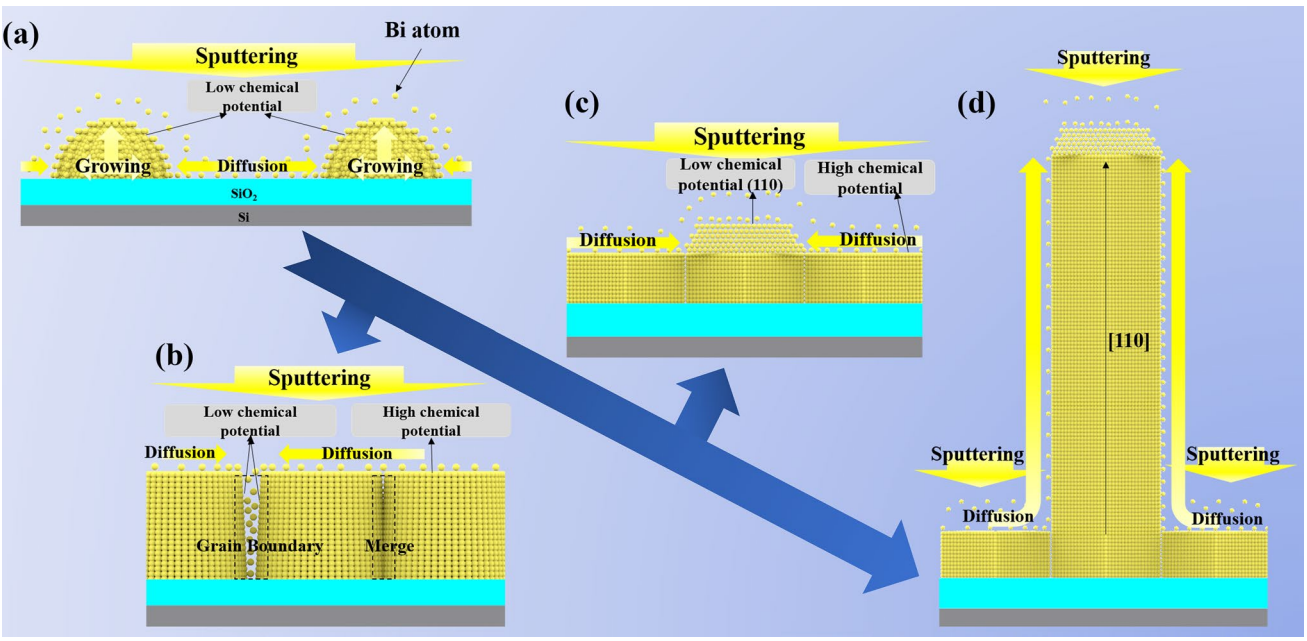

Fig. 8 Schematic illustration of the growth mechanism during the sputtering process. **a** The bismuth clusters formation at the initial stage of bismuth film formation. **b** The formation of bismuth film. **c** The sprouting of bismuth nanowire. **d** The growth of bismuth nanowire

collective adatoms are piled up and condensed at stable position to form single crystalline burgeons. As the burgeons growing up, the diffusive bismuth adatoms not only need to travel along the film surface but also experience the journey along the nanowire's sidewall within the diffusion length λ_{NW} at nanowire's sidewall as shown in Fig. 8d. Further sputtering, the nanowires keep growing and almost saturates as the lengths reach to λ_{NW}. The adatoms supplied from nanowire's sidewall and tip are much smaller than that supplied from film surface for a large area difference between the sidewall and film surface. As a result, the growth rate of nanowire falls sharply and the regime is termed as nanowire ripening stage. In temperature-varying group, the mean length of bismuth nanowires increases linearly as the substrate temperature increase. This can be attributed to the viscidity of bismuth adatoms closes to that of viscous fluid for a stronger attraction between adatoms and solid surface than that between atoms in vapor. Therefore, the relationship between diffusion coefficient and temperature follows Stokes–Einstein equation (Einstein 1905), $D = kT/6\pi\mu r$, where k presents Boltzmann constant, μ the viscidity of solution, r the radius of diffusive particle, and T the temperature. Nevertheless, the bismuth adatoms can also be treated as relatively slow-moving vapor on the solid surface due to the special state between condensation and evaporation. In consequence, as discussed in pressure-varying group, the sputtering pressure impacts the diffusion coefficient of bismuth adatoms in a manner of negative linear tendency. The weaker influence of pressure as compared to that of ideal vapor $D \propto 1/p$ deduced by Maxwell–Boltzmann distribution, possibly owing to languorous motion of adatoms. In power-varying group, the mean length of nanowires increases with sputtering power within 17.16 W and decreases at higher power. For the increase regime, the higher power supplies more adatoms for diffusion to accelerate the growth of nanowire. However, the acceleration slows down as larger atom flux from sputtering hampers the diffusion of adatoms. The adatoms condensed more quickly due to greater impingement of atoms from the sputtering flux, resulting in shorter diffusion distance. Even worse, as the attenuation of nanowire's growth rate induced by increase impingement surpasses the promotion from the quantity increase in adatoms, the mean length of bismuth nanowires declines. In addition, mean diameters of bismuth nanowires in time-varying and power-varying groups are revealed to be linearly proportional to the sputtering time and power, respectively, indicating a linear relationship with respected to the quantity of deposited atoms. Moreover, the trends of mean diameters with variables in temperature-varying and pressure-varying groups also present diffusion coefficient-related growth mechanism. Consequently, the growth mechanism of bismuth nanowire by sputtering is demonstrated to be surface diffusion governed by difference of surface chemical potential.

Besides, another two possible mechanisms for the growth of nanowire are reasonably precluded. As for screw dislocation-driven nanowire growth mechanism, although the high anisotropic crystal growth in the formation of nanowire and the presence of cone like tip are typical features of screw dislocation driven growth mechanism, however, none of any dislocation line is observed by diffraction contrast transmission electron microscope images (Bierman et al. 2008). Therefore, screw dislocation-driven nanowire growth mechanism cannot account for the formation of nanowires in our work. For self-catalyzed growth mechanism, the exclusion can be made by theoretical calculations. Provided that the growth of bismuth nanowires was induced by self-catalyzed growth, the tips of the nanowires must be liquid in such scale. Therefore, the determination of whether the tips are melted or not is vital. The melting point T_m of a definite scale bismuth droplet is governed by $T_m = (1 - \eta S/V)T_0$ (Olson et al. 2005), where η is related to surface energies of the solid and liquid phases and experimentally determined as 0.23 nm (Floro et al. 2002; Allen et al. 1986), S/V is the surface area to volume ratio and T_0 the bulk melting temperature. The free surface of the melted particle is defined as $S = \int_0^\theta \mathrm{d}S = 2\pi R^2 \int_0^\theta \sin\theta \mathrm{d}\theta = 2\pi R^2(1 - \cos\theta)$ here R is the radius of the particle, and θ is the angle between OA and OB, as depicted in left inset of Fig. 9b. And the volume of the particle is defined as $V = \pi R^3 \int_0^\theta \left(\cos^2\theta - 1\right)d(\cos\theta) = \pi R^3(2/3 + 1/3\cos^3\theta - \cos\theta)$, therefore, $S/V = 2(1 - \cos\theta)/R(2/3 + 1/3\cos^3\theta - \cos\theta)$. The θ dependence of T_m with varied particle radius is plotted in Fig. 9a. The wire radius O'B = 57 nm and O'A = 39 nm, therefore, the radius of small particle on the bismuth nanowire is calculated to be ~ 61 nm, from which corresponding θ to be ~ 1.2. In our experiments, the radius of the grown bismuth nanowire falls in the range of 20–100 nm, as the pink region depicted in Fig. 9b. In this range, the respected melting temperature is all above the sputtering temperature more than 100 K, definitely precluding the self-catalyzed mechanism.

Conclusions

In summary, the morphology, crystallinity, and growth mechanism of bismuth nanowire by sputtering are thoroughly investigated. The morphology evolution of bismuth nanowire growth by sputtering is captured for the first time, and three corresponding growth stages are discriminated as film formation, nanowire-hillock growing, and nanowire ripening. With sputtering time increase, a non-uniform growth in the nanowire's axis direction, where

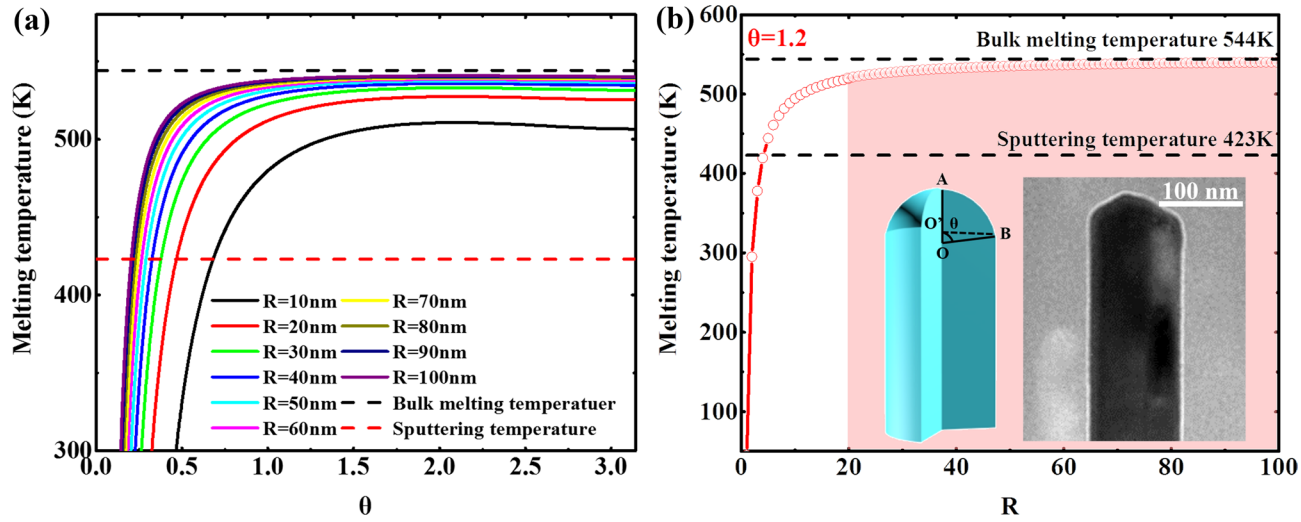

Fig. 9 The dependence of melting temperature on **a** θ, and **b** small particle radius at $\theta = 1.2$, the insets are schematic illustration of 3D nanowire model and TEM image of bismuth nanowire

the growth rate is fast at the initial stage and slow at the later stage of the nanowire growing regime, and a uniform growth in the nanowire's radial direction are demonstrated. Besides, both the mean length and mean diameter of the nanowires are approximately increase uniformly with the rise of substrate temperature. Moreover, increasing the sputtering pressure hampers the growth of bismuth nanowire either in length or radius. Furthermore, increasing the sputtering power within a moderate range promotes the growth of nanowire while attenuation takes place as the power further increase. However, the mean diameter of the nanowires is supposed to extend linearly with the increase in power. In addition, the crystallinity of the bismuth nanowire is proofed to be single crystalline with preferred axis orientation [110], which is consistent with the result from BFDH principle. Accordingly, a reasonable growth model based on surface diffusion is structured rigorously. The bismuth adatom diffusion is supposed to be motivated directly by the adatom concentration gradient, which is induced by the difference of surface chemical potential among surfaces. Besides, stress driven, screw dislocation driven, and self-catalyzed mechanisms are precluded separately based on the theoretical and experimental data. The thoroughly understanding of growth mechanism is fundamental and necessary for fabrication of size-controllable bismuth nanowires. Furthermore, the growth mechanism of bismuth nanowire we proposed in this work may be available for the formation of other low dimensional structure materials by merely sputtering. Therefore, further investigations of novel properties of bismuth nanowires and other low dimensional material in a more cost-effective and simple way are feasible.

Acknowledgements This work is supported by the National Natural Science Foundation of China (61474094) and National Basic Research Program of China (2013CB632103). The authors wish to thank Yunyong Zhang for the help of SEM tests and Shuhong Zhang for the assist of TEM and SAED characterization.

Compliance with ethical standards

Conflict of interest There are no conflicts to declare.

References

Allen GL, Bayles RA, Gile WW, Jesser WA (1986) Small particle melting of pure metals. Thin Solid Films 144:297–308. https://doi.org/10.1016/0040-6090(86)90422-0

Benalcazar WA, Andrei Bernevig B, Hughes TL (2017) Quantized electric multipole insulators. Science 357:61–66. https://doi.org/10.1126/science.aah6442

Bierman MJ, Lau YKA, Kirt AV et al (2008) Dislocation-driven nanowire growth and Eshelby twist. Science 320:1060–1063. https://doi.org/10.1126/science.1157131

Cao S, Guo C, Wang Y et al (2009) Template-catalyst-free growth of single crystalline Bismuth nanorods by RF magnetron sputtering method. Solid State Commun 149:87–90. https://doi.org/10.1016/j.ssc.2008.10.003

Chason E, Sheldon BW, Freund LB et al (2002) Origin of compressive residual stress in polycrystalline thin films. Phys Rev Lett 88:4. https://doi.org/10.1103/PhysRevLett.88.156103

Cheng YT, Weiner AM, Wong CA et al (2002) Stress-induced growth of bismuth nanowires. Appl Phys Lett 81:3248–3250. https://doi.org/10.1063/1.1515885

Docherty R, Clydesdale G, Roberts KJ, Bennema P (1991) Application of Bravais–Friedel–Donnay–Harker, attachment energy and ising models to predicting and understanding the morphology of molecular crystals. J Phys D Appl Phys 24:89–99. https://doi.org/10.1088/0022-3727/24/2/001

Drozdov IK, Alexandradinata A, Jeon S et al (2014) One-dimensional topological edge states of bismuth bilayers. Nat Phys 10:664–669. https://doi.org/10.1038/NPHYS3048

Einstein A (1905) Uber d4e von der rnolekuZarh%net4schem Theorie der WUrme geforderte Bewegumg vow in ruhenden P Z ikss4ykeitem. Ann Phys 322:549–560. https://doi.org/10.1002/andp.19053220806

Floro JA, Chason E, Cammarata RC, Srolovitz DJ (2002) Physical origins of intrinsic stresses in Volmer–Weber thin films. MRS Bull 27:19–25. https://doi.org/10.1557/mrs2002.15

Lee HY, Wu BK, Chern MY (2013) Schottky photodiode fabricated from hydrogen-peroxide-treated ZnO nanowires. Appl Phys Express 6:2–5. https://doi.org/10.7567/APEX.6.054103

Li L, Zhang Y, Li G, Zhang L (2003) A route to fabricate single crystalline bismuth nanowire arrays with different diameters. Chem Phys Lett 378:244–249. https://doi.org/10.1016/S0009-2614(03)01264-8

Li C, Kasumov A, Murani A et al (2014) Magnetic field resistant quantum interferences in Josephson junctions based on bismuth nanowires. Phys Rev B Condens Matter Mater Phys 90:1–5. https://doi.org/10.1103/PhysRevB.90.245427

Lin YM, Sun X, Dresselhaus M (2000) Theoretical investigation of thermoelectric transport properties of cylindrical Bi nanowires. Phys Rev B Condens Matter Mater Phys 62:4610–4623. https://doi.org/10.1103/PhysRevB.62.4610

Liu K, Chien C, Searson P (1998) Finite-size effects in bismuth nanowires. Phys Rev B Condens Matter Mater Phys 58:R14681–R14684. https://doi.org/10.1103/PhysRevB.58.R14681

Liu XY, Zeng JH, Zhang SY et al (2003) Novel bismuth nanotube arrays synthesized by solvothermal method. Chem Phys Lett 374:348–352. https://doi.org/10.1016/S0009-2614(03)00730-9

Murakami S (2006) Quantum spin hall effect and enhanced magnetic response by spin-orbit coupling. Phys Rev Lett 97:1–4. https://doi.org/10.1103/PhysRevLett.97.236805

Murani A, Kasumov A, Sengupta S et al (2017) Ballistic edge states in Bismuth nanowires revealed by SQUID interferometry. Nat Commun 8:1–20. https://doi.org/10.1038/ncomms15941

Olson EA, Efremov MY, Zhang M et al (2005) Size-dependent melting of Bi nanoparticles. J Appl Phys 97:034304. https://doi.org/10.1063/1.1832741

Schindler F, Cook AM, Vergniory MG et al (2018a) Higher-order topological insulators. Sci Adv 4:eaat0346. https://doi.org/10.1126/sciadv.aat0346

Schindler F, Wang Z, Vergniory MG et al (2018b) Higher-order topology in bismuth. Nat Phys 14:918–924. https://doi.org/10.1038/s41567-018-0224-7

Shim W, Ham J, Il Lee K et al (2009) On-film formation of Bi nanowires with extraordinary electron mobility. Nano Lett 9:18–22. https://doi.org/10.1021/nl8016829

Stanley SA, Stuttle C, Caruana AJ et al (2012) An investigation of the growth of bismuth whiskers and nanowires during physical vapour deposition. J Phys D Appl Phys 45:435304. https://doi.org/10.1088/0022-3727/45/43/435304

Tian Y, Guo CF, Guo S et al (2012) Bismuth nanowire growth under low deposition rate and its ohmic contact free of interface damage. AIP Adv 2:012112. https://doi.org/10.1063/1.3679086

Woo RL, Gao L, Goel N et al (2009) Kinetic control of self-catalyzed indium phosphide nanowires, nanocones, and nanopillars. Nano Lett 9:2207–2211. https://doi.org/10.1021/nl803584u